Solvent Extraction Research and Development, Japan, **Vol. 30, No 1, 81 – 93 (2023)**

Variation of Extraction Yield and Droplet Size during Emulsification Solvent Extraction of Wet-Process Phosphoric Acid

Yuqing CAO*

College of Materials and Chemistry & Chemical Engineering, Chengdu University of Technology, Chengdu 610059, PR China

** Corresponding author. cmm_wd@126.com*

(Received June 15, 2022; Accepted October 31, 2022)

This research focuses on emulsification solvent extraction for purifying wet-process phosphoric acid. The effects of various parameters, including stirring speed, phase ratio and emulsification time on the extraction yield and droplet size distribution were investigated. The optimal conditions were determined. The influence of time and physical properties of solvent on average droplet diameter was fitted by dimensional analysis. The results showed that the mathematical model has a strong agreement with the experimental data. This model was reliable to predicting the droplet size in different conditions of manufacturing emulsion.

1. Introduction

Phosphoric acid (PA) is widely used in food, fertilizers, pharmaceuticals, electronics and other industries as an important raw material for chemical intermediate [1]. In these industrial applications, the purity requirement for PA, especially for wet-process phosphoric acid (WPA), is extremely high. Some techniques for purifying PA have recently been developed, such as crystallization [2,3], ion exchange [4,5], adsorption [6,7], and solvent extraction [8-10]. Among these, solvent extraction is an ideal purifying approach because of its low energy consumption, comparatively simpler production technology and equipment, and ease of automating batch production. The conventional solvent extraction method uses agitation or reciprocating sieve plate column to mix oil and aqueous phase [11]. However, because this method takes a long time to reach the extraction equilibrium, it requires a large amount of extractant and a lot of floor space.

To optimize the solvent extraction process, it is necessary to increase the contact area and improve the mass transfer efficiency of the two phases [12]. Emulsification solvent extraction (ESE) [13] is currently the most successful approach for achieving the desired effects. During the emulsion-making process, the two phases form an emulsion with a large interfacial area by mechanical forces. When compares to the traditional extraction methods, ESE can provide a larger specific surface area for mass transfer, which improves the extraction efficiency, shortens the residence time, and reduces energy consumption and equipment investment. Therefore, ESE has been widely used in the chemical industry, metallurgy [14], medical [15], food [16] and other fields.

Many factors have an effect on the process of ESE [17]. Luo et al. [18] investigated the effects of the D2EHPA volume fraction, the phase volume ratio, the initial pH of NaH_2PO_4 solution, the stirring time and

agitation speed on the emulsification solvent extraction efficiencies of Fe^{3+} from sodium dihydrogen phosphate. Kara et al. [19] researched the effects of pH, the EDTA concentration, the ultrasonic extraction time, and the centrifugation time on the extraction efficiency of trace elements from edible oils by ultrasound-assisted emulsification. Najafi et al. [20] investigated the effects of the extraction solvent volume, the disperser solvent volume, the concentration of chelating agent, the salt effect and the extraction time on the extraction of inorganic selenium in different environmental water samples. Zou et al. [21] studied the extraction yield of PA and drop size of the emulsion affected by phase ratio, stirring speed, extraction time, extractant and phosphoric acid concentration. These studies focus more on furnace-process phosphoric acid with only a few impurities. Purification of WPA, which contains many impurities, is got more and more attention in places where high-grade phosphate rocks are scarce. However, few researchers have studied how the extraction process of WPA is influenced by various factors.

In this paper, extractant tributyl phosphate (TBP) was used to extract PA from the WPA dilute solution. A water-in-oil (W/O) emulsion of this extraction system was formed with high-speed stirring, wherein the dilute solution is the dispersed phase and TBP is the continuous phase [22]. The effects of stirring speed (N), phase ratio (φ) and emulsification time (t) on P_2O_5 extraction yield were investigated. The droplet size distribution (DSD) and average droplet size (d_{43}) of emulsion have two significances on this process. On the one hand, it reflects the strength of the emulsion production process, and indirectly reflects whether the mass transfer of the process is sufficient. On the other hand, DSD serves as both a guide for the subsequent demulsification, and a microscopic characterization of the effectiveness of the demulsification procedure. Therefore, DSD and d_{43} of emulsion under different conditions were measured to evaluate the emulsifying effectiveness. A model was established by dimensional analysis to correlate d_{43} and the above parameters and predict d_{43} during emulsification process. The operating conditions of emulsification extraction can be optimized by this model, so that the extraction yield can reach the maximum quickly and d_{43} will not be too small.

2. Experimental

2.1 Materials

WPA was supplied by Sanhuan Chemical Co. Ltd. (Yunnan, China). Its main components are listed in Table 1. TBP (purity ≥98.5%) was produced by Shifang Zhongcui Chemical Co. Ltd. (Sichuan, China). Deionized water was used to dilute raw acid and produced by a making-water machine (Aquapro Industrial Co., Ltd., ABZ1-1001-P, Taiwan, China).

Table 1. Main components of WPA.

Component	P_2O_5	SO_4^{2-}	Fe^{3+}	F^-
Mass fraction /%	47.2	3.56	0.97	0.54

2.2 Emulsification extraction procedure

The experiments were carried out at the temperature (T) of 323 ± 0.2 K. Appropriate volumes of TBP and raw acid were accurately measured with a total volume of 500 mL and poured into a high beaker, which was placed in a water bath pot for preheating at least 10 min. Then the high shear emulsification machine's (Youyi Instruments Co., Ltd., Fluko JRJ-300-I, Shanghai, China) stirring speed was adjusted to

the required setting to agitate. Agitating was stopped after reaching a different extraction time, and a homogenization emulsion was obtained. A 150 mL sample of the emulsion was transferred to a particle size analyzer (Sympatec GmbH, OPUS, Clausthal-Zellerfeld, Germany) immediately to observe the variation and evolution of droplet size. Two phases were separated after a period of time. The oil phase (extract) was obtained on the upper layer, while the aqueous phase (raffinate) was obtained on the lower layer. To calculate the extraction yield, the mass of the two phases and phosphorus content were measured. Throughout the procedure, a steady temperature was maintained. All of the experiments were repeated at least twice and the results were averaged.

2.3 Analysis

The phosphorus contents of the raw acid and the aqueous phase are determined by the quinoline phosphomolybdate gravimetric method [23].

Extraction yield is calculated by the following equation:

$$E = \frac{\omega_r(P_2O_5) - \omega_a(P_2O_5)}{\omega_r(P_2O_5)} \times 100\% \quad (1)$$

where E is extraction yield of PA, $\omega_r(P_2O_5)$ and $\omega_a(P_2O_5)$ are the mass of phosphorus pentoxide (P_2O_5) in the raw acid and the aqueous phase, respectively.

d_{43} and DSD were measured with the particle size analyzer. DSD is expressed as the density distribution ($q_3\ln(x)$) and calculated by the following equation [24]:

$$q_3\ln(x) = \frac{[Q_3(x_i + \Delta x) - Q_3(x_i)] \times 2.3}{\ln[(x_i + \Delta x)/x_i]} \quad (2)$$

where x_i is the lower limit of the divided range of DSD, Δx is the length of the divided range of DSD, 2.3 is equal to ln10, Q_3 is the function of volume cumulative distribution, as given by the defining eq. (3). d_{43} is calculated by eq. (4) [25]:

$$Q_3(x_i) = \frac{\text{Fraction of quantity of particles in the interval}}{\text{Total quantity of the particles}} \quad (3)$$

$$d_{43} = \sum_{j=1}^{n} d_j^4 \Big/ \sum_{j=1}^{n} d_j^3 \quad (4)$$

where d_j is droplet diameter.

3. Results and discussion

3.1 Traditional extraction method

In order to ensure the data accuracy of the extraction equilibrium of the experiment system, variation of preliminary stirring time of the traditional extraction is performed by moderate heating in water. The difference in physical property and concentration between the two phases determines the extraction yield: in different states, the extraction equilibrium is predicted to have a similar regularity with the yield.

In this experiment (stirred, not emulsified), the phase ratio (φ, O/A) refers to the volume ratio of oil phase and aqueous phase, and the value was set to 4:1. The mixture is placed in a constant temperature (323 K) water bath for 10 minutes. Then it was stirred at a low speed (400 rpm) to avoid emulsification and set a different extraction time (stirring time). Following the cessation of stirring, the two phases were separated and weighed quickly, and the phosphorus content is determined to calculate the extraction yield. The results

are presented in Figure 1. The extraction yield increased significantly as the extraction time increased. It should be noted that the traditional extraction has an equilibrium time of up to 30 min, implying that the extraction will take a long time to complete.

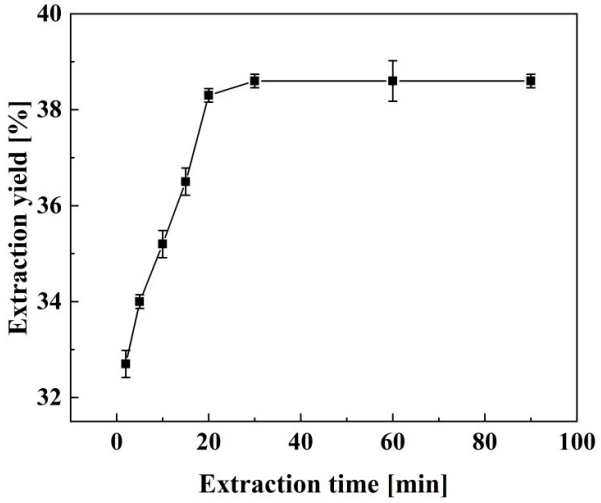

Figure 1. Effect of extraction time on the extraction yield under the conditions: N = 400 rpm, φ = 4:1, T = 323 K.

3.2 Effect of stirring speed on the extraction yield and DSD

It can be observed from the data in Figure 2 that there is essentially no variation in extraction yield as the range of stirring speed (N) increased from 1000 to 6000 rpm. The other emulsion-making parameters: t was 30 s and φ was 4:1. That means the mixed solution was dispersed into a multitude of minute droplets by the mechanical emulsion, hence increasing their contact surface. As a result, even if N of the ESEs in this study was quite different, they may have all reached extraction equilibrium in the same amount of time.

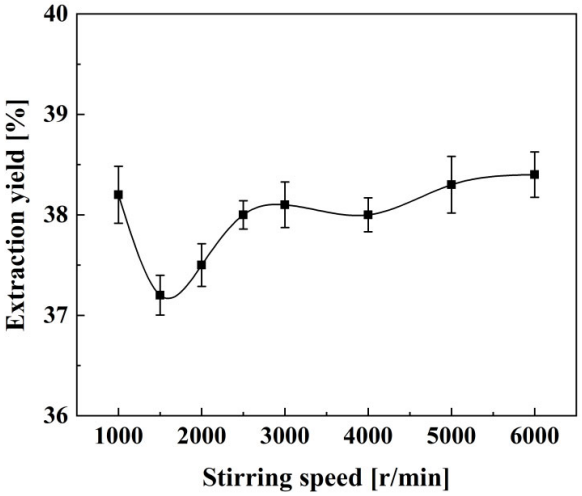

Figure 2. Effect of N on the extraction yield under the conditions: t = 30 s, φ = 4:1, T = 323 K.

The variation of density distribution of droplets (by density distribution) with the increasing N is shown in Figure 3. At low speeds, the density distribution curve is monomodal, but as N increases, it progressively becomes bimodal, with smaller droplets emerging. The higher N, the more small droplets exist. Increasing the mixing energy provides additional energy to break large-sized droplets into small-sized daughter droplets [26]. The droplets are stretched into threads before breaking up [27] and producing smaller droplets, resulting in the bimodal distribution. Agitation can generate small droplets, but it also promotes the droplet flocculation and coalescence, both of which are intensified with a higher N. The rates of droplet formation, flocculation and coalescence are dynamically balanced at a certain N. The droplet size is restricted by the action of agitation, which is impossibly infinitesimal. The cumulative proportion of the small droplets number improves slightly as N increases. Meanwhile the DSD curve offsets to the left.

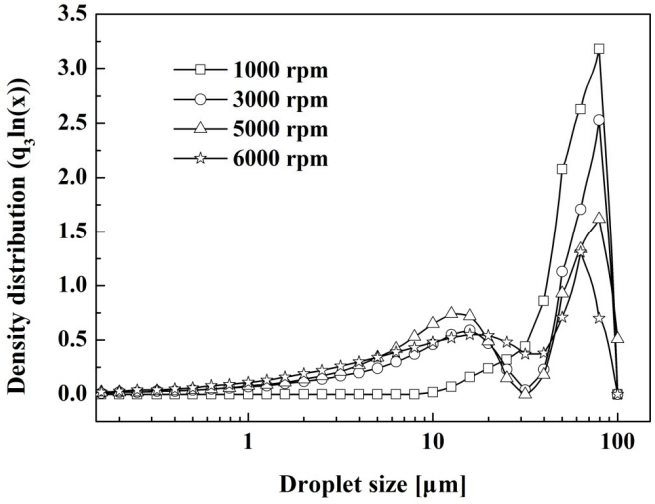

Figure 3. The evolution of DSD at different N under the conditions: t = 30 s, φ = 4:1, T = 323 K.

3.3 Effect of phase ratio on the extraction yield and DSD

φ also plays a crucial role in terms of the overall extraction yield of the emulsion. The effect of φ ranged from 1:1 to 6:1 on the extraction yield, as presented in Figure 4. The other conditions: t is 30 s and N is 1000 rpm. It is obvious that the best result is obtained when φ is high. However, as extractant volume increases, the improved mass transfer dynamics promote the balanced reaction; the emulsion becomes more stable, which exacerbates the difficulty of phase separation. Therefore, in light of the aforementioned problems and circulation volume of the extractant, the appropriate φ is determined to be 4:1, which is in the case of a high extraction yield.

As φ increases from 3:1 to 6:1, oil phase volume fraction increases and the distribution changes from bimodal to stable monomodal (Figure 5). As φ increases, the moisture content decreases, and the interfacial tension decreases, resulting in an increase in coalescence rate among small droplets and the formation of a stable larger distribution [28]. The final variation in DSD is very little because the total volume maintains constant in this experiment, with little change in the oil phase as φ increases to 4:1 or higher.

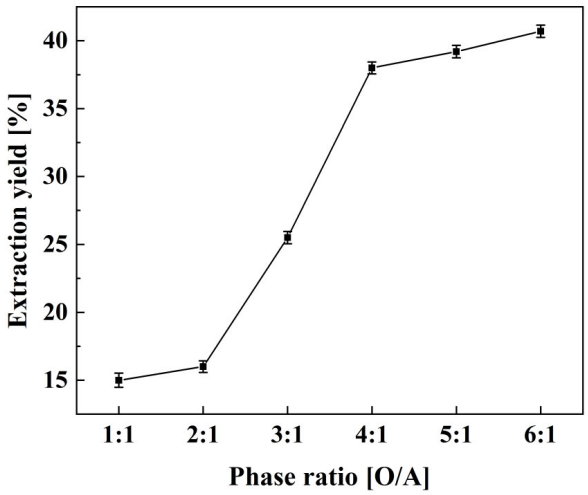

Figure 4. Effect of φ on the extraction yield under the conditions: t = 30 s, N = 1000 rpm, T = 323 K.

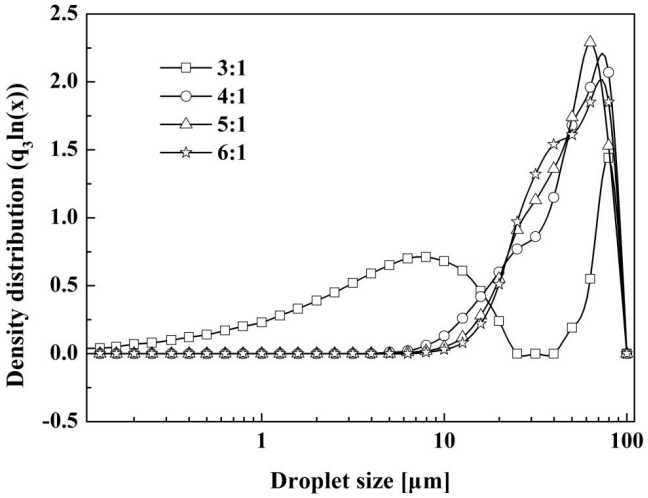

Figure 5. The evolution of DSD of different φ under the conditions: t = 30 s, N = 1000 rpm, T = 323 K.

3.4 Effect of emulsification time on the extraction yield and DSD

In order to determine the minimum time to achieve extraction equilibrium while reducing the system's input power, the effect of t on the extraction yield was investigated (Figure 6). t ranges from 15 to 240 s under the other conditions: φ = 4:1, N = 1000 rpm and T = 323 K. As seen in Figure 6, the curve is on the rise before 30 s, then varies slightly over a period of 40 to 240 s. It means that the extraction system has reached equilibrium when t equals 30 s. Increasing t will increase energy consumption and may increase the mutual combination of TBP and impurities in the dispersed phase, thereby reducing its ability to extract phosphoric acid. As a result, 30 s was selected as the shortest t that can reach equilibrium. Comparing Figures 1 and 6, it is found that the emulsification extraction technology can indeed make the extraction reach

an equilibrium state in a short time, which greatly reduces the process time. In addition, the circulation amount of the extractant in the extraction tank can be reduced, thereby saving space and material cost.

The stability of emulsion increases over t. When t is too short, the formation of oil-water interface is unstable. The dispersed phase is unevenly scattered and easily formed a large number of irregularly shaped water bags that are significantly larger than the stable droplets, reducing the mass transfer ability. However, too long t causes increased energy dissipation and emulsion stability. DSD changed little within the scope of t in this experiment (Figure 7), which has a d_{43} of 50 μm, indicating that the emulsification process was completed [29].

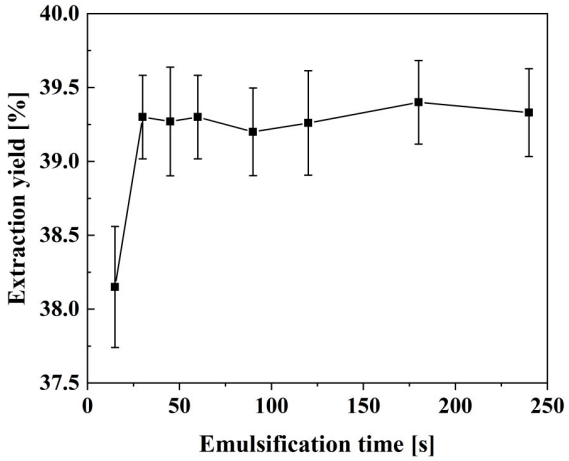

Figure 6. Effect of t on the extraction yield under the conditions: φ = 4:1, N = 1000 rpm, T = 323 K.

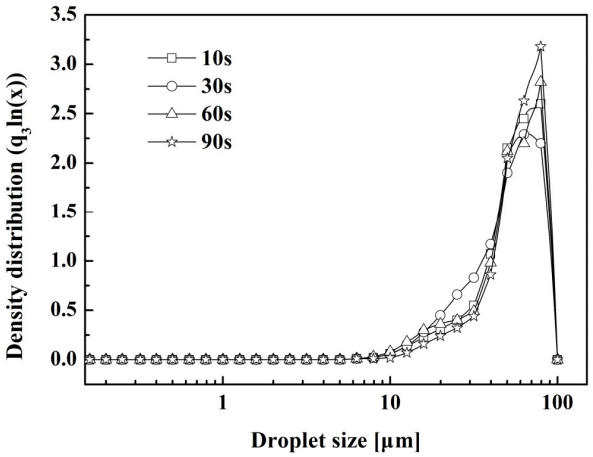

Figure 7. The evolution of DSD of different t under the conditions: φ = 4:1, N = 1000 rpm, T = 323 K.

3.5 Variation of DSD with settling time

Following emulsification under the conditions: t = 30 s, φ = 4:1, N = 1000 rpm and T = 323 K, about 150 mL emulsion was transferred immediately to the particle size analyzer to observe the variation of DSD with settling time (t_s) (Figure 8). With t_s increasing from 5 to 55 min, the number of the small droplets in the range of 5–20 μm reduces to zero, and the change of DSDs range from 20–100 μm is little. This phe-

nomenon can be explained by two reasons. First, Brownian motion exists in the emulsion, and because small droplets have a higher curvature, they have a higher chemical potential and solubility. As t_s increases, small droplets coalesce into large droplets and are disappeared [30]. Second, the measuring area of the analyzer may be fixed, resulting in measured droplets always being suspended in this area and changing slightly. However, it reflects DSDs of the "rigid particles" when the droplets reach dynamic equilibrium in suspension [31,32]. It is also the phase separation's technical bottleneck. As shown in Figure 8, d_{43} of the "rigid particles" is about 52 μm, and the ranges of these DSD curves are about 20 to 100 μm.

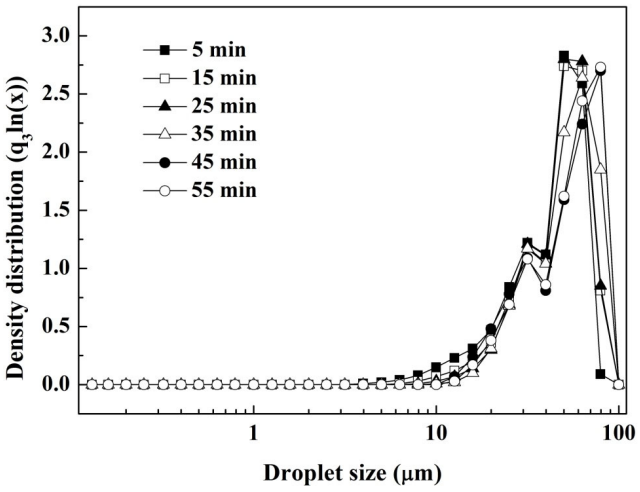

Figure 8. The variation of DSD with t_s: t = 30 s, φ = 4:1, N = 1000 rpm and T = 323 K.

3.6 Mathematical modeling for predicting the average droplet diameter

Dimensionless analysis has been widely applied in chemical industry to reduce the experiment times and simplify the experiment process. The theoretical foundation of dimensional analysis is Buckingham Pi theorem, the details of which can be found in the literature [33-36]. In this experiment, the average droplet diameter (d_{43}) was correlated with stirring speed (N), phase ratio (φ), emulsification time (t), settling time (t_s), and density of dispersed phase (ρ_d). These independent variables correlate to the following equation:

$$\phi(\rho_d,\ N, t,\ t_s,\ \varphi,\ d_{43}) = 0 \tag{5}$$

The first step is to determine the dimensions of both dependent and independent variables (Table 2). Knowing the outer diameter of stirring paddle (0.07 m), N can be converted to linear velocity (v), which is calculated by eq. (6). Measuring the density (ρ_d and ρ_c) and volume (V_d and V_c) of the two equilibrium phases, the density of the mixture (ρ_m) can be calculated, which is calculated by eq. (7).

$$v = \frac{N \times 3.14 \times 0.07}{60} \tag{6}$$

$$\rho_m = \frac{\rho_d V_d + \rho_c V_c}{V_d + V_c} \tag{7}$$

Table 2. The dimensions of parameters.

Variables	Typical units	Dimensions [a]
Density of dispersed phase (ρ_d)	kg/m^3	$L^{-3}M^1T^0$
Linear velocity (v)	m/s	$L^1M^0T^{-1}$
Emulsification time (t)	s	$L^0M^0T^1$
Settling time (t_s)	s	$L^0M^0T^1$
Density of the mixture (ρ_m)	kg/m^3	$L^{-3}M^1T^0$
Average droplet diameter (d_{43})	m	$L^1M^0T^0$

[a] L-length, M-mass, T-time

Secondly, three independent dimensionless groups are formed according to the Buckingham Pi theorem:

$$\pi_1 = \frac{t_s}{t}, \quad \pi_2 = \frac{d_{43}}{vt}, \quad \pi_3 = \frac{\rho_m}{\rho_d} \tag{8}$$

Finally, using eq. (8) to cover for eq. (5), it can be shown that a further form of eq. (5) may present as:

$$\phi\left(\frac{t_s}{t}, \frac{d_{43}}{vt}, \frac{\rho_m}{\rho_d}\right) = 0 \tag{9}$$

Only three parametric spaces are used to describe the process, and d_{43} can be expressed by the following equation:

$$d_{43} = v \times t \times f\left(\pi_1, \pi_3\right) \tag{10}$$

To utilize data adequately, it's necessary to get the concrete form of eq. (10). Due to large amounts of data used, only the data under the conditions in this manuscript are listed in Table 3. The content of phosphoric acid in the two phases is not very high, and TBP is poorly water-soluble during the extraction process. However, the precipitation of impurities and the loss result in a slight decrease in the volume of the two equilibrium phases.

The nonlinear regression equation is obtained by mathematical analysis software, and through the way of comparing experimental with calculated values to find the best-fitting equation. The final form can be compressed to the following expression:

$$d_{43} = vt\left(a + b\pi_1 + c{\pi_1}^2 + d{\pi_1}^3 + e{\pi_1}^4 + f\pi_3 + g{\pi_3}^2 + h{\pi_3}^3\right) \times 10^{-6} \tag{11}$$

where a = 1.504; b = 1.632×10^{-1}; c = -9.344×10^{-2}; d = 2.248×10^{-2}; e = -1.509×10^{-3}; f = 1.416×10^{1}; g = 4.493×10^{1}; h= 4.621×10^{1}.

The comparison of d_{43} between the calculated and experimental data is shown in Figure 9**,** with the coefficient of determination (R^2) of 0.935, indicating a good alignment in the microcosmic field. It is possible to match and predict d_{43} for most conditions of ESE.

Table 3. Linear velocity, densities of the two equilibrium phases and mixture under different conditions.

Emulsification time (s)	Stirring speed (rpm)	Phase ratio (φ)	Density of dispersed phase (kg/m^3)	Density of continuous phase (ρ_c, kg/m^3)	Linear velocity (m/s)	Density of mixture (kg/m^3)
30	1000	4:1	1569	1020	3.66	1129
30	2000	4:1	1587	1020	7.33	1132
30	3000	4:1	1595	1020	10.99	1134
30	4000	4:1	1603	1020	14.65	1135
30	5000	4:1	1610	1020	18.32	1137
30	6000	4:1	1615	1020	21.98	1138
30	1000	1:1	1569	1032	3.66	1301
30	1000	2:1	1550	1028	3.66	1201
30	1000	3:1	1535	1026	3.66	1153
30	1000	5:1	1483	1015	3.66	1092
30	1000	6:1	1468	1008	3.66	1073
10	1000	4:1	1574	1017	3.66	1127
45	1000	4:1	1569	1020	3.66	1128
60	1000	4:1	1569	1020	3.66	1128
75	1000	4:1	1569	1020	3.66	1129
90	1000	4:1	1569	1020	3.66	1128

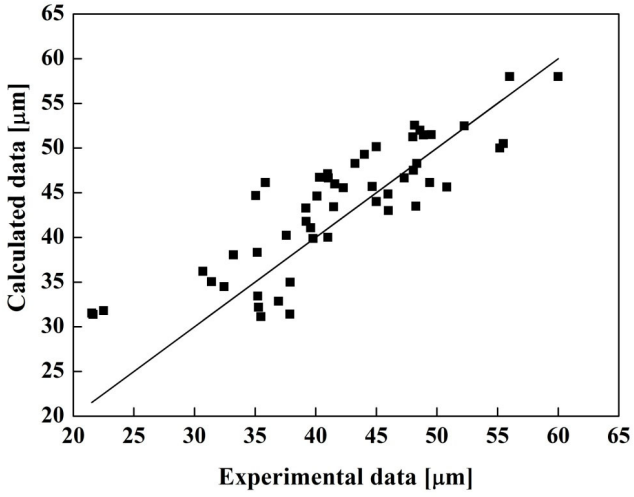

Figure 9. Comparison between experimental and calculated data.

As indicated by the form of π_1 and π_3 (eq. (8)), π_1 is the related parameter of time, and π_3 is that of physical properties of solvent. The variation of d_{43} with π_3 is illustrated in Figure 10. For all the cases shown in Figure 10, d_{43} slips from a beginning rising trend and then levels off in the end as π_3 increases, which can be explained for two reasons. On one hand, droplets with different sizes have different settling velocities driven by gravity and buoyancy. According to Hadamard-Rybczynski equation [37], the

settling velocity of large droplets is greater than that of small droplets. The droplets collide at random and high frequency with settlement, but the general rule is that small droplets coalesce into large droplets, and large droplets coalesce into larger droplets. And then these larger droplets break up to form two phases, so the large droplets first increase and then decrease until there are some rigid small droplets that are less likely to coalesce. On the other hand, large droplets might catch smaller ones as they pass through the measurement area, so some larger droplets are measured first, followed by smaller ones.

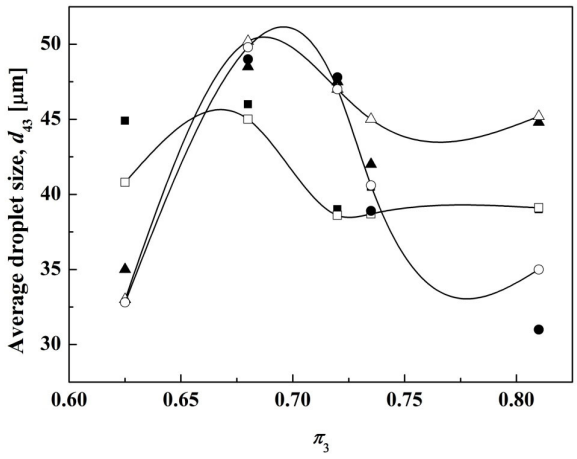

Figure 10. Effect of π_3 on d_{43}. (■ π_1=2 Exp., □ π_1=2 model, ▲ π_1=5 Exp., △ π_1=5 model, ● π_1=10 Exp., ○ π_1=10 model)

Figure 11 displays π_1 corresponding to d_{43}. The longer t_s, the more likely it is that coalescence will occur, which contributes the formation of larger droplets. However, the effect of t on the droplets size shows a inverse relationship. The solution generates a large number of small droplets with increasing t. The number of small droplets reduces following coalescence from the perspective of DSDs, but that of large ones does not always increase, indicating that the forms of coalescence are multitudinous.

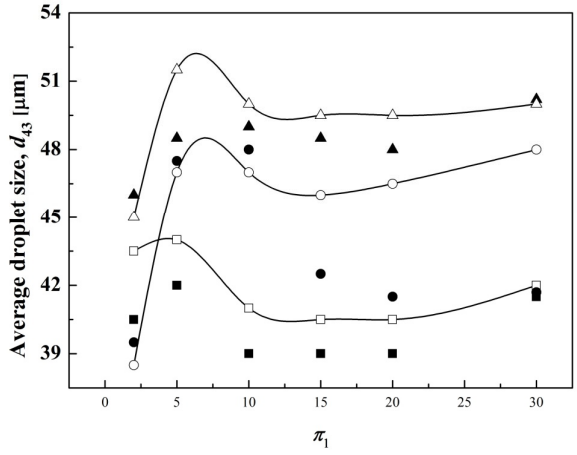

Figure 11. Effect of π_1 on d_{43}. (■ π_3 = 0.625 Exp., □ π_3 =0.625 model, ▲ π_3 =0.686 Exp., △ π_3 =0.686 model, ● π_3=0.718 Exp., ○ π_3=0.718 model)

4. Conclusion

In this work, experiments have been performed to investigate and quantify the effect of process parameters and formulation variables on the extraction yield and the relative size of droplets. The optimal conditions are as follows: stirring speed of 1000 rpm, phase volume ratio of 4:1, and emulsification time of 30 s. As the emulsification time and rate increase, the average droplet diameter decreases until it reaches a limit size. It was clearly demonstrated that DSD is more concentrated and the size is larger under optimal conditions. Application of the dimensional analysis has been allowed to identify the above-mentioned parameters. A process model based on the relationship between key variables is established, and it predicts the diameter of droplets successfully during the emulsifying process.

References

1) A. V. Slack, "*Phosphoric Acid*", Marcel Dekker Inc, New York (1968).
2) K.-J. Kim, *Chem. Eng. Technol.*, **29**, 271-276 (2006).
3) B. M. Wang, J. Li, Y. B. Qi, X. H. Jia, J. H. Luo, *Cryst. Res. Technol.*, **47**, 1113-1120 (2012).
4) J. E. Salmon, H. R. Tietze, *J. Chem. Soc.*, 2324-2326 (1952).
5) M. B. C. Elleuch, M. B. Amor, G. Pourcelly, *Sep. Purif. Technol.*, **51**, 285-290 (2006).
6) S. Zermane, A. H. Meniai, *Energy Procedia*, **18**, 888-895 (2012).
7) J. M. Lewis, R. A. Kydd, *J. Catal.*, **132**, 465-471 (1991).
8) S. Reuna, A. Väisänen, *Chem. Pap.*, **76**, 417-425 (2022).
9) C. Ye, J. Li, *J. Chem. Technol. Biotechnol.*, **88**, 1715-1720 (2013).
10) A. Hannachi, D. Habaili, C. Chtara, A. Ratel, *Sep. Purif. Technol.*, **55**, 212-216 (2007).
11) A. Stella, K. H. Mensforth, T. Bowser, G. W. Stevens, H. R. C. Pratt, *Ind. Eng. Chem. Res.*, **47**, 3996-4007 (2008).
12) Z. G. Zhang, Y. L. Ma, S. C. Ye, J. Li, B. H. Zhong, *Chem. Ind. Eng. Prog.*, **30**, 1632-1636 (2011).
13) M.-K. Yeh, A. G. A. Coombes, P. G. Jenkins, S. S. Davis, *J. Controlled Release*, **33**, 437-445 (1995).
14) H. M. Elsayed, E. A. Fouad, N. M. T. El-Hazek, A. K. Khoniem, *J. Radioanal Nucl. Chem.*, **298**, 1763-1775 (2013).
15) F. Espitalier, B. Biscans, C. Laguérie, *Chem. Eng. J.*, **68**, 103-114 (1997).
16) C. K. Siew, P. A. Williams, *J. Agric. Food Chem.*, **56**, 4164-4171 (2008).
17) Y. Cao, Y. Jin, J. Li, D. Zou, X. Chen, *Sep. Purif. Technol.*, **158**, 387-395 (2016).
18) J. H. Luo, J. Li, X. X. Duan, *J. Ind. Eng. Chem.*, **19**, 727-731 (2013).
19) D. Kara, A. Fisher, S. Hill, *Food Chem.*, **188**, 143-148 (2015).
20) N. M. Najafi, H. Tavakoli, Y. Abdollahzadeh, R. Alizadeh, *Anal. Chim. Acta*, **714**, 82-88 (2012).
21) D. Zou, Y. Jin, J. Li, Y. Cao, X. Li, *Sep. Purif. Technol.*, **172**, 242-250 (2017).
22) Y. Cao, Y. Jin, J. Li, K. Zhou, F. Zhuge, *Sep. Sci. Technol.*, **55**, 811-821 (2020).
23) H. N. Wilson, *Analyst*, **76**, 65-76 (1951).
24) "*OPUS Manual 7.0*", ed. by Sympatec GmbH System-Partikel-Technik (2006).
25) A. Koocheki, R. Kadkhodaee, *Food Hydrocolloids*, **25**, 1149-1157 (2011).
26) G. Narsimhan, D. Ramkrishna, J. P. Gupta, *AIChE J.*, **26**, 991-1000 (1980).
27) C. Liu, M. Li, C. Liang, W. Wang, *Chem. Eng. Sci.*, **102**, 622-631 (2013).

28) W. L. Kang, J. H. Li, X. Q. Zhao, *Oil-Gas Field Surf. Eng.*, **24**, 11-12 (2005).
29) S.-Y. Tan, R. F. Tabor, L. Ong, G. W. Stevens, R. R. Dagastine, *Soft Matter*, **8**, 3112-3121 (2012).
30) Y. Liao, D. Lucas, *Chem. Eng. Sci.*, **65**, 2851-2864 (2010).
31) Z. Li, D. Harbottle, E. Pensini, T. Ngai, W. Richtering, Z. Xu, *Langmuir*, **31**, 6282-6288 (2015).
32) A. Gupta, M. Sbragaglia, *Phys. Rev. E*, **90**, 023305 (17 pages) (2014).
33) E. Buckingham, *Phys. Rev.*, **4**, 345-376 (1914).
34) P. W. Bridgman, "*Dimensional Analysis*", Yale University Press, New Haven (1922).
35) H. L. Langhaar, "*Dimensional Analysis and Theory of Models*", John Wiley & Sons Inc., New York (1951).
36) W. P. Liang, "*The Foundation of Emulsion Science and Technology*", Science Press, Beijing (2001).
37) T. Miyahara, S. Yamanaka, *J. Chem. Eng. Jpn.*, **26**, 297-302 (1993).